Resource Allocation and Performance Analysis of Cellular-assisted OFDMA Device-to-Device Communications

Yuan Kai, *Member, IEEE*, Junyuan Wang, *Member, IEEE*,
Huiling Zhu, *Senior Member, IEEE*, and Jiangzhou Wang, *Fellow, IEEE*

***Abstract*—Resource allocation of cellular-assisted device-to-device (D2D) communication is very challenging when frequency reuse is considered among multiple D2D pairs within a cell, as intense inter D2D interference is difficult to tackle and generally causes extremely large signaling overhead for channel state information (CSI) acquisition. In this paper, a novel resource allocation framework for cellular-assisted D2D communication is developed with low signaling overhead while maintaining high system capacity. By utilizing the spatial dispersion property of D2D pairs, a geography-based sub-cell division strategy is proposed to divide the cell into multiple sub-cells and D2D pairs within one sub-cell are formed into one group. Then, sub-cell resource allocation is performed independently among sub-cells without the need of any prior knowledge of inter D2D interference. Under the proposed resource allocation framework, a tractable approximation for the inter D2D interference modelling is obtained and a computationally efficient expression for the average ergodic sum capacity of the cell is derived. The expression further allows us to obtain the optimal number of sub-cells, which is an important parameter for maximizing the average ergodic sum capacity of the cell. It is shown that with small CSI feedback, system capacity can be improved significantly by adopting the proposed resource allocation framework, especially in dense D2D deployed systems.**

***Index Terms*—Device-to-Device (D2D) communications, resource allocation, intra-cell interference, cellular networks.**

I. Introduction

The tremendous growth of multimedia applications (e.g. video content delivery, online gaming, etc.) leads to strong demands for high data-rate and low latency services in future wireless mobile communications. Device-to-device (D2D) communication underlaying the cellular system, referred to as cellular D2D communication, is expected to be one of the key technologies to improve user data rate and network throughput, while reducing latency and energy consumption for data transmission [1]–[3]. Under the assistance of cellular base station (BS), cellular D2D communication allows two nearby cellular users to form a D2D pair and communicate with each other directly without traversing the BS or core network, thus improving the transmit quality significantly due to short transmission distance [4].

In cellular systems, orthogonal frequency division multiple access (OFDMA) has been widely adopted for multi-user transmissions. Based on the property inherited from orthogonal frequency division multiplexing (OFDM) which transforms the frequency selective fading channel into multiple flat fading subcarriers, high system capacity can be achieved by exploring multi-user diversity when adaptively allocating the subcarriers to multiple users [5], [6]. Since all the cellular users within one cell need to communicate with the central BS, subcarriers cannot be reused by multiple cellular users within one cell due to the formidable strong intra-cell interference. By contrast, for cellular D2D underlaid OFDMA systems, both transmitters and receivers of the D2D pairs are spatially distributed within the cell and the transmission distance of a formed D2D pair is very small compared to the cell radius. Therefore, reusing same subcarriers among multiple D2D pairs and/or between D2D pairs and cellular users could improve the overall system capacity, if mutual interference among multiple D2D pairs and cellular users is managed carefully.

Extensive efforts have been made to address the resource allocation problem along with interference coordination for cellular D2D underlaid OFDMA systems [7]–[12]. To guarantee the quality of service requirements of both cellular and D2D users, [7] focused on the design of proper admission access control of D2D users. The quantitative trade-off between energy efficiency and delay in D2D underlaid cellular networks was derived in [8], with the help of fractional programming and the Lyapunov optimization techniques. Based on graph theory, [9] and [10] introduced a sub-optimal resource allocation scheme by modelling the interference among multiple D2D pairs and cellular users as an interference graph. Game theory has also been employed from the economic perspective in [11] and [12] to design distributed resource allocation algorithms.

Note that in the aforementioned research works, licensed spectrum is assumed to be reused among multiple D2D pairs and one cellular user within one cell to maximize the overall system capacity. In a large-scale D2D underlaid cellular system with hundreds of geographically distributed D2D pairs, severe cross D2D and cellular interference would significantly degrade the performance of cellular users, thus limiting the frequency reuse among D2D pairs and cellular users, which further impairs the spectral efficiency. Moreover, the

Manuscript received January 24, 2018; revised July 5, 2018; October 23, 2018; accepted October 26, 2018. The associate editor coordinating the review of this paper and approving it for publication was J. Lee. *(Corresponding author: Junyuan Wang)*

Y. Kai, H. Zhu and J. Wang are with the School of Engineering and Digital Arts, University of Kent, Canterbury, CT2 7NT, U.K. (e-mail: {yk69, h.zhu, j.z.wang}@kent.ac.uk).

J. Wang is with the Department of Computer Science, Edge Hill University, Ormskirk, L39 4QP, U.K. (e-mail: junyuan.wang@edgehill.ac.uk).

computational complexity and extra interference measurement overhead for joint resource allocation of D2D pairs and cellular users would be prohibitively high [13]. To minimize the impact of D2D communication on existing cellular resource allocation, in this paper, we focus on the orthogonal sharing mode as mentioned in [14], where dedicated spectrum is allocated to the D2D pairs within the cell. As a consequence, only inter D2D interference exists among the D2D pairs using the same spectrum within one cell, and interference coordination between D2D pairs and cellular users is not needed anymore.

In contrast to the resource allocation for cellular OFDMA systems, which is generally decoupled into *orthogonal subcarrier assignment* to each user and *power allocation* to each subcarrier [5], joint consideration of *non-orthogonal subcarrier assignment* among multiple D2D pairs and power allocation is required to achieve optimal system performance, e.g. system capacity, for cellular D2D underlaid OFDMA systems, as each subcarrier can be reused by multiple D2D pairs in the cell. Due to the non-convexity of the received signal to interference plus noise ratio (SINR) at each device and the binary constraints of subcarrier allocation, the resource allocation of D2D communication is generally formed as a non-convex mixed-integer problem, which was proved to be strongly NP-hard [15]. The most commonly used technique to tackle the non-convexity is the standard Lagrange dual relaxation [15]–[17]. It was shown in [16] that zero duality gap can be achieved when the number of subcarriers grows to infinitely large. With a limited number of subcarriers, either sequential convex programming or successive convex approximation were adopted in [18]–[20] to approximate the original non-convex resource allocation problem. Although sub-optimal system performance of D2D communications could be obtained based on different optimization frameworks, perfect knowledge of channel state information (CSI) between the transmitter and receiver of any D2D pair was generally assumed at the BS. Such inevitable high signalling overhead and computational complexity make the resource allocation algorithms difficult to be implemented in practical systems with the growing density of D2D communications [21]. How to establish a scalable resource allocation framework for cellular D2D communication systems is a key challenge that needs to be addressed.

Basically, the spatial dispersion property of D2D pairs, which means that the distance between any two D2D pairs could be relatively large compared to the distance of a D2D pair, is the root cause of spectrum reusing among D2D pairs in one cell, as the inter D2D interference is largely determined by the distance-dependent path loss. In [22], by considering that subcarriers should not be reused in a small area to avoid the strong interference, interference limited area was introduced to manage the interference from cellular users to D2D pairs with some predetermined interference to signal ratio threshold at D2D receivers. It is shown that significant D2D gain can be achieved with low complexity. However, such spatial dispersion property of D2D pairs has not been used to assist the resource allocation of D2D communications in previous works. In this paper, a novel resource allocation framework is proposed for D2D communication underlaid OFDMA systems to utilize the spatial dispersion property of D2D pairs effectively. With the objective of achieving high spectral efficiency with low complexity, the resource allocation is decoupled into two stages. First, a simple geography-based D2D sub-cell division strategy is proposed to divide the D2D pairs within one cell into multiple groups. Specifically, the coverage of one single cell is divided into L small areas under symmetric hexagonal topology, referred to as sub-cells, and the D2D pairs located within one sub-cell are set into one group. In the second stage, dedicated subcarriers for cellular D2D communications are orthogonally assigned to the D2D pairs in one sub-cell to avoid the strong intra sub-cell interference, whereas the subcarriers are reused among different sub-cells to enhance the overall spectral efficiency.

Thanks to the sub-cell division strategy, the inter D2D interference is strictly limited between the D2D pairs in different sub-cells. Nevertheless, the signalling overhead for the CSI measurement of the interference channels between D2D pairs in different sub-cells could still be high, if sub-cell division and resource allocation of multiple sub-cells are jointly considered. Hence, we propose to perform *orthogonal* subcarrier assignment and power allocation, referred to as sub-cell resource allocation, to maximize the ergodic sum capacity for the D2D pairs in each sub-cell independently without the need of the CSIs of the inter D2D interference channels. Furthermore, the number of sub-cells L, which is a key system parameter for the sub-cell division strategy, largely affects the inter D2D interference and thus the system sum capacity with the proposed resource allocation framework. Since the inter D2D interference closely depends on the positions of D2D pairs, instead of maximizing the instantaneous system sum capacity, we aim to investigate the optimal number of sub-cells that maximizes the *average ergodic sum capacity* of cellular D2D underlaid OFDMA systems in this paper, where the ergodic sum capacity is averaged over D2D pairs' locations.

The main contributions of this paper are summarized as follows:

- By utilizing the spatial dispersion property of D2D pairs in cellular systems, we propose a resource allocation framework that enfolds sub-cell division and sub-cell resource allocation. In particular, with the proposed geography-based sub-cell division strategy, the joint non-orthogonal subcarrier assignment and power allocation problem is decomposed into a number of independent orthogonal subcarrier assignment and power allocation problems, which can reduce the computational complexity and signalling overhead of CSI measurement significantly.
- We investigated two representative sub-cell resource allocation schemes, i.e., Best Subcarrier CSI-based Resource allocation (BSCR) scheme and Subcarrier Achievable capacity-based Resource allocation (SAR) scheme, with respect to the individual transmit power constraint of each D2D pair. For the sake of comparison, closed-form expressions of ergodic sum capacities with both BSCR scheme and SAR scheme are derived as functions of the number of D2D pairs and the number of subcarriers, which are verified by extensive simulation results.

- We further analysed the inter D2D interference between D2D pairs under our proposed resource allocation framework thoroughly, based on which, the analytical expression of average ergodic sum capacity is derived as a function of the number of sub-cells that is a vital system parameter for the sub-cell division strategy. Simulation results corroborate the accuracy of the optimal number of sub-cells obtained from the analysis and show that substantial system capacity gains can be achieved by the proposed resource allocation framework.

The rest of this paper is organized as follows. In Section II, the system model for the cellular D2D underlaid OFDMA system is introduced along with the proposed sub-cell division strategy. The sub-cell resource allocation algorithms and corresponding sum capacities under the single sub-cell structure are investigated in Section III. The sum capacity under multiple sub-cell structure and the effect of the number of sub-cells are further investigated in Section IV. Finally, conclusions are summarized in Section V.

II. System Model

To make the rest of this paper easy to follow, the frequently used notations are summarized in Table I.

TABLE I
Notations of System Parameters

Parameter	Definition
$\mathcal{K}$	Set of D2D pairs distributed in the cell following a PPP
$\mathcal{N}$	Set of subcarriers for D2D communications
R	Radius of the cell coverage area
L	Number of sub-cells based on the hexagonal sub-cell division structure
R_L	Radius of each sub-cell
$\mathcal{K}_l$	Set of D2D pairs in sub-cell l according to the hexagonal sub-cell division structure
P_{max}	Maximum transmit power of the D2D transmitter
$P_{k,n}$	Transmit power of $D2D_k$ on subcarrier n
d_{k_l}	Distance between the transmitter and the receiver of $D2D_{k_l}$
$d_{k_{l'},k_l}$	Distance between the transmitter of $D2D_{k_{l'}}$ and the receiver of $D2D_{k_l}$
α	Path loss exponent
$g_{k_{l'},k_l,n}$	Channel gain from the transmitter of $D2D_{k_{l'}}$ to the receiver of $D2D_{k_l}$ on subcarrier n
$I^c_{k_l,n}$	Cumulative inter D2D interference received at $D2D_{k_l}$ on subcarrier n
$C_{k_l,n}$	Achievable data rate of $D2D_{k_l}$ on subcarrier n
C_{TOT}	Sum capacity of the D2D pairs in the cell
$\bar{C}_{TOT}$	Average ergodic sum capacity of the D2D pairs in the cell

Consider an OFDMA-based single cell system underlaid by D2D communications. As shown in Fig.1(a), a set of K active D2D pairs, denoted as $\mathcal{K} = \{1, \cdots, K\}$, are located in the coverage area of one base station (BS). The kth D2D pair, $D2D_k$, is formed by a transmit device and a receive device, called transmitter k and receiver k, respectively. In this model, the circular area with radius R is denoted as the coverage region of the BS centred at the origin. It is assumed that the D2D transmitters are distributed in the whole $\mathbb{R}^2$ plane following a homogeneous Poisson Point Process (PPP) Φ_A with density λ_A, and the receiver k associated with transmitter k is located uniformly on the circle centred by transmitter k with distance d_k, which is assumed to be one in this paper.[1] Then the average number of D2D pairs in the cell, denoted as $\bar{K}$, is given by $\bar{K} = \pi\lambda_A R^2$. The maximum transmit power of each D2D device is assumed to be limited to P_{max}.

To avoid the cross interference between D2D pairs and cellular users, a set of N dedicated subcarriers, denoted as $\mathcal{N} = \{1, \cdots, N\}$, are assigned for D2D communications. Each subcarrier can be reused among multiple D2D pairs within the cell in order to increase the system spectral efficiency. As a consequence, inter D2D interference exists among the D2D pairs sharing the same subcarrier. Specifically, for the D2D pair $D2D_k$, the potential inter D2D interference on subcarrier n comes from the transmitter of any $D2D_{k'}$, $k' \in \mathcal{K} \setminus \{k\}$. Note that the interference only exists when the same subcarrier is reused by $D2D_k$ and $D2D_{k'}$. Hence, non-orthogonal subcarrier assignment is performed to determine the set of D2D pairs that can share the same subcarrier. In addition, as each device has the maximum transmit power P_{max}, the power allocation on the assigned subcarriers to each D2D pair is inextricably interwoven with the non-orthogonal subcarrier assignment. Thus, joint consideration of non-orthogonal subcarrier assignment and power allocation is required for resource allocation of cellular D2D underlaid OFDMA systems. However, the optimization problem is unfortunately proven to be NP-hard [15], which requires unaffordable computing capability at the BS to trace the optimal resource allocation result. Moreover, it induces a massive amount of signalling overhead for D2D channel measurement and feedback, especially when the number of D2D pairs K is large.

It has been shown in [22] that when a subcarrier is shared by two nearby D2D pairs, strong inter D2D interference would degrade the performance of both D2D pairs significantly. In other words, inter D2D interference can be efficiently reduced by preventing the D2D pairs within a small area from reusing the same subcarrier. Therefore, in order to avoid strong inter D2D interference, we propose to divide the cell into multiple disjoint small areas, which are referred to as sub-cells in this paper, and orthogonally allocate the N subcarriers to the D2D pairs within the same sub-cell. That is, N subcarriers can be reused among different sub-cells only.

A. Sub-cell Division Strategy

As the D2D transmitters are assumed to be uniformly distributed in the cell, without loss of generality, for any specific D2D pair $D2D_k$, the distance between any other D2D transmitter and the receiver of $D2D_k$ follows an independent and identical distribution. By assuming the location information of all the D2D pairs are perfectly obtained at the D2D discovery stage [23], a simple geography-based sub-cell division strategy is proposed. Specifically, the single cell is considered as a J-tier symmetrical hexagonal sub-cell structure, as shown in

[1]Note that the admission access control is generally required to form D2D pairs prior to the resource allocation of D2D communications. Due to the limited maximum transmit power of each device, the distance of a formed D2D pair is very small compared to the cell radius. For the sake of simplicity, the distance of each D2D pair is assumed to be one in this paper.

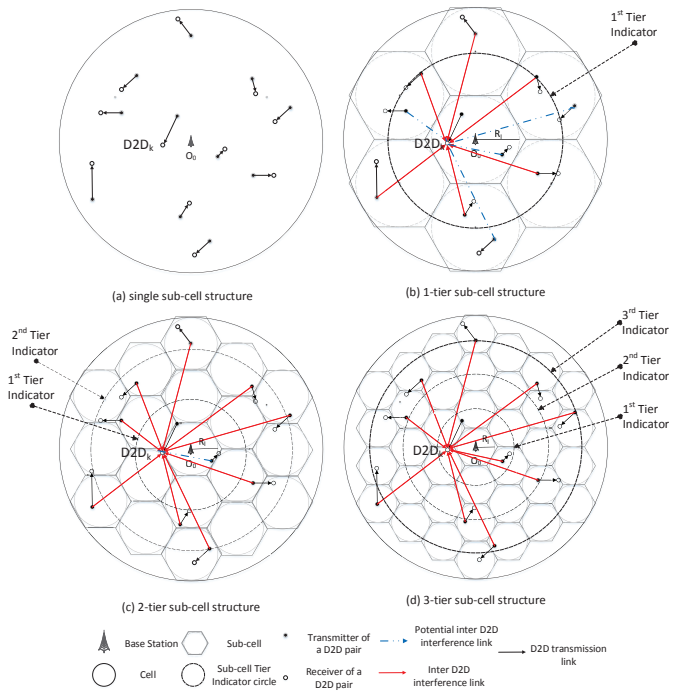

Fig. 1. System model of cellular-assisted D2D communications with hexagonal sub-cell division strategy.

Figs. 1(b)-1(d). By taking the central sub-cell as the reference sub-cell, we denote its neighbouring sub-cells as the 1st tier sub-cells, which are crossed by the 1st tier circle. Similarly, the jth tier is formed by the outer neighbouring sub-cells of the $(j-1)$th tier sub-cells. Based on the geographic characteristic of a J-tier hexagonal structure, the single cell is divided into a total of $L = 3 \cdot J \cdot (1+J)+1$ sub-cells. Each sub-cell can be then approximated as a circle area with radius R_L [24], and indexed from one to L. The sub-cell radius can be obtained as

$$R_L = \frac{R}{1+2 \cdot J} = \sqrt{\frac{3}{4L-1}} \cdot R. \tag{1}$$

With the sub-cell division, K D2D pairs are divided into L groups, where group l includes a set of D2D pairs, $\mathcal{K}_l$, located within the lth sub-cell. Note that when $L = 1$, all the K D2D pairs are in the same group and there is no inter D2D interference, while the number of interference links increases with the number of sub-cells for any specific D2D pair $D2D_k$, as shown in Fig. 1. Hence, it can be seen intuitively that the cumulative inter D2D interference received at $D2D_k$ depends on the number of sub-cells L.

B. Signal Model

In this paper, the channel of each subcarrier is assumed to remain the same during a resource allocation period. If subcarrier n is allocated to $D2D_{k_l}$ in sub-cell l, the received signal at the receiver of $D2D_{k_l}$ can be written as

$$y_{k_l,n} = \sqrt{P_{k_l,n}} \cdot g_{k_l,n} \cdot s_{k_l,n} + \underbrace{\sum_{\substack{l'\neq l \\ l'=1}}^{L} \sum_{k_{l'} \in \mathcal{K}_{l'}} \sqrt{P_{k_{l'},n}} \cdot g_{k_{l'},k_l,n} \cdot s_{k_{l'},n}}_{\text{Interference}} + z_{k_l,n}, \tag{2}$$

where $s_{k_l,n}$ is a complex scalar representing the information signal from $D2D_{k_l}$ on subcarrier n with $\mathbb{E}[|s_{k_l,n}|^2] = 1$, and $P_{k_l,n}$ denotes the transmit power of $D2D_{k_l}$ on subcarrier n. $z_{k_l,n} \sim CN(0,\sigma^2)$ is the additive white Gaussian noise (AWGN) at the receiver of $D2D_{k_l}$. The channel gain from the transmitter of $D2D_{k_{l'}}$ in sub-cell l' to the receiver of $D2D_{k_l}$ is denoted as $g_{k_{l'},k_l,n}$,[2] given by

$$g_{k_{l'},k_l,n} = \iota_{k_{l'},k_l} \cdot h_{k_{l'},k_l,n}, \tag{3}$$

where $h_{k_{l'},k_l,n}$ is the small-scale fading and assumed to be an independent and identically distributed (i.i.d.) Rayleigh random variable with zero mean and unit variance. $\iota_{k_{l'},k_l}$ represents the path loss coefficient, given by

$$\iota_{k_{l'},k_l} = {d_{k_{l'},k_l}}^{-\frac{\alpha}{2}}, \tag{4}$$

where $d_{k_{l'},k_l}$ is the distance from $D2D_{k_{l'}}$ to $D2D_{k_l}$, and α is the path loss exponent.

The achievable data rate of $D2D_{k_l}$ on subcarrier n can then be expressed as

$$C_{k_l,n} = B \cdot \log_2\left(1 + \frac{P_{k_l,n} \cdot |g_{k_l,n}|^2}{I^c_{k_l,n} + \sigma^2}\right), \tag{5}$$

where B denotes the bandwidth of one subcarrier. $I^c_{k_l,n}$ is the cumulative inter D2D interference received at $D2D_{k_l}$ on subcarrier n, which can be obtained according to (2) as

$$I^c_{k_l,n} = \sum_{\substack{l'\neq l \\ l'=1}}^{L} \sum_{k_{l'} \in \mathcal{K}_{l'}} P_{k_{l'},n} \cdot \left|g_{k_{l'},k_l,n}\right|^2. \tag{6}$$

C. Problem Formulation

With the geography-based sub-cell division strategy proposed in Section II-A, the sum capacity of K D2D pairs within the cell can be seen as the sum capacity of L sub-cells.

For the sake of clarity, we introduce the subcarrier assignment indicator denoted as $\omega_{k_l,n}$, where $\omega_{k_l,n} = 1$ indicates that subcarrier n is allocated to $D2D_{k_l}$, otherwise, $\omega_{k_l,n} = 0$, for all $k_l \in \mathcal{K}_l$ and $n \in \mathcal{N}$. The sum capacity of the cell under L sub-cell structure is then given by

$$C_{TOT} = \sum_{l=1}^{L} \sum_{k_l \in \mathcal{K}_l} \sum_{n \in \mathcal{N}} \omega_{k_l,n} \cdot B \cdot \log_2\left(1 + \frac{P_{k_l,n}\left|g_{k_l,n}\right|^2}{\sum_{\substack{l'\neq l \\ l'=1}}^{L} \sum_{k_{l'} \in \mathcal{K}_{l'}} \omega_{k_{l'},n} P_{k_{l'},n}\left|g_{k_{l'},k_l,n}\right|^2 + \sigma^2}\right). \tag{7}$$

[2]For simple notation, the channel gain on subcarrier n between the transmitter and receiver of $D2D_{k_l}$, $g_{k_l,k_l,n}$ is denoted as $g_{k_l,n}$. In the rest of the paper, the subscript of any random variable between the transmitter and receiver of one D2D pair is simplified in the same manner.

The joint optimization problem of sub-cell division, subcarrier assignment and power allocation can be formulated as

$$\max_{L,\ \{\omega_{k_l,n}\},\ \{P_{k_l,n}\}} C_{TOT} \tag{8}$$

$$s.t. \qquad \omega_{k_l,n} \in \{0,1\}, \quad \forall\ k_l \in \mathcal{K}_l,\ n \in \mathcal{N}, l = 1, \cdots, L; \tag{8a}$$

$$\sum_{k_l \in \mathcal{K}_l} \omega_{k_l,n} \leqslant 1, \quad \forall\ n \in \mathcal{N}, \quad l = 1, \cdots, L; \tag{8b}$$

$$\sum_{n \in \mathcal{N}} P_{k_l,n} \leqslant P_{max}, \quad \forall\ k_l \in \mathcal{K}_l, \quad l = 1, \cdots, L; \tag{8c}$$

where constraint (8a) indicates the integer property of the subcarrier assignment indicator and constraint (8b) indicates that the subcarrier n can be allocated to at most one D2D pair within each sub-cell, which implies that a subcarrier cannot be reused within one sub-cell. Constraint (8c) shows that the total transmit power of a D2D pair is limited by the maximum transmit power P_{max}.

It can be clearly seen from (8) that based on the sub-cell division strategy, there are three sets of parameters to be optimized to achieve the maximum sum capacity, i.e., the number of sub-cells L and the resource allocation results $\{\omega_{k_l,n}\}_{k_l \in \mathcal{K}_l, n \in \mathcal{N}}$, $\{P_{k_l,n}\}_{k_l \in \mathcal{K}_l, n \in \mathcal{N}}$ for each sub-cell $l = 1, \cdots, L$. As the resource allocation of L sub-cells are correlated with each other due to the inter D2D interference, the CSI between any D2D pairs in the cell, $\{g_{k',k,n}\}_{k' \in \mathcal{K}, k \in \mathcal{K}, n \in \mathcal{N}}$, are required at the BS to achieve the optimal resource allocation, leading to $\mathcal{O}(K^2N)$ signalling overhead for CSI measurement.

In order to alleviate the high signalling overhead, in this paper, sub-cell resource allocation is proposed to perform orthogonal subcarrier assignment and power allocation for the D2D pairs within each sub-cell regardless of the inter D2D interference. As a result, the signalling overhead for CSI measurement is significantly reduced from $\mathcal{O}(K^2N)$ to $\mathcal{O}(KN)$, since only the CSI of each D2D pair, $\{g_{k,n}\}_{k \in \mathcal{K}, n \in \mathcal{N}}$, is needed. On the other hand, it is noted that the ergodic sum capacity is decisively affected by the inter D2D interference, which varies with the locations of D2D pairs. Instead of optimizing the number of sub-cells for each realization of D2D locations, we are interested in optimizing the number of sub-cells, $\hat{L}$, that maximizes the average ergodic sum capacity of the system over the positions of all D2D pairs, which will be studied in Section IV.

III. Sum Capacity under Single Sub-cell Structure

As discussed in Section II, the subcarriers are orthogonally assigned to the D2D pairs within the same sub-cell regardless of interference. In this section, a special case under the single sub-cell structure (i.e. $L = 1$, as shown in Fig. 1(a)) is considered, where no inter D2D interference exists. The sub-cell resource allocation, including orthogonal subcarrier assignment and power allocation, is investigated first and the ergodic sum capacity is then studied in section III-B.

A. Single Sub-cell Resource Allocation

With the objective of maximizing the sum capacity of the K D2D pairs in the single sub-cell, the optimization problem for the resource allocation in (8) can be reformulated as

$$\max_{\{\omega_{k,n}\},\ \{P_{k,n}\}} C = \sum_{k \in \mathcal{K}} \sum_{n \in \mathcal{N}} B \cdot \omega_{k,n} \cdot \log_2 \left(1 + \frac{P_{k,n} \left|g_{k,n}\right|^2}{\sigma^2}\right) \tag{9}$$

$$\text{s.t.} \qquad \omega_{k,n} \in \{0,1\}, \forall\ k \in \mathcal{K},\ n \in \mathcal{N}; \tag{9a}$$

$$\sum_{k \in \mathcal{K}} \omega_{k,n} \leqslant 1,\ \forall\ n \in \mathcal{N}; \tag{9b}$$

$$\sum_{n \in \mathcal{N}} P_{k,n} \leqslant P_{max},\ \forall\ k \in \mathcal{K}. \tag{9c}$$

To handle the resource allocation problem of single sub-cell in (9), two strategies are considered in this paper, respectively.

Firstly, multi-user diversity is generally exploited for subcarrier assignment in OFDMA systems to maximize the sum capacity by assigning each subcarrier to the user with the highest channel gain among all users [5]. This strategy can be adopted to solve the multiple-D2D resource allocation problem in (9), which is referred to as *Best Subcarrier CSI-based Resource allocation (BSCR)* in this paper. That is, each subcarrier is allocated to the D2D pair with the best CSI. After subcarrier assignment, a set of subcarriers assigned to $D2D_k$, $\mathcal{N}_k$ with cardinality $N_k = |\mathcal{N}_k|$, is determined. For each D2D pair, P_{max} is assigned to its allocated N_k subcarriers by using water-filling algorithm [25].

However, as the subcarrier assignment and power allocation are tackled separately in the BSCR scheme, a large number of subcarriers might be allocated to one D2D pair, which leads to low transmit power per subcarrier due to the limited transmit power per device and thus degrades the sum capacity. A joint subcarrier assignment and power allocation scheme called *Subcarrier Achievable capacity-based Resource allocation (SAR)* was proposed in [26] to solve this problem.

For SAR scheme, as an initial step, it is assumed that equal power allocation is applied to the set of N_k subcarriers, $\mathcal{N}_k$, allocated to $D2D_k$. Thus, the transmit power for $D2D_k$ on each allocated subcarrier is given by $P_{k,n_k} = \frac{P_{max}}{N_k}, \forall n_k \in \mathcal{N}_k$, and the sum capacity of the cell is

$$C = \sum_{k \in \mathcal{K}} C_k\left(\mathcal{N}_k\right), \tag{10}$$

where $C_k\left(\mathcal{N}_k\right)$ denotes the capacity of $D2D_k$, and can be shown as

$$C_k(\mathcal{N}_k) = \sum_{n_k \in \mathcal{N}_k} C_{k,n_k} = \sum_{n_k \in \mathcal{N}_k} B \log_2 \left(1 + \frac{P_{max} \left|g_{k,n_k}\right|^2}{N_k \cdot \sigma^2}\right). \tag{11}$$

Given the set of subcarriers allocated to $D2D_k$, $\mathcal{N}_k$, and a set of unallocated subcarriers $\mathcal{N}_u$, if one of the unallocated subcarriers $n \in \mathcal{N}_u$ is to be allocated to $D2D_k$, i.e. $\mathcal{N}_k$ being replaced by $\mathcal{N}_k \bigcup \{n\}$, the increment of the sum capacity ΔC is equal to the increment of the capacity of $D2D_k$, $\Delta C_{k,n}$,

$$\Delta C = \Delta C_{k,n} = C_k(\mathcal{N}_k \cup \{n\}) - C_k\left(\mathcal{N}_k\right). \tag{12}$$

Then, for a given $\mathcal{N}_k$, whether an unallocated subcarrier n can be allocated to $D2D_k$ depends on whether its capacity increment $\Delta C_{k,n}$ is the maximum value of $\{\Delta C_{k,n}\}_{k\in\mathcal{K},n\in\mathcal{N}_u}$. That is, in each subcarrier assignment step, a subcarrier n^* will be allocated to $D2D_{k^*}$ with the largest $\Delta C_{k^*,n^*}$, i.e., $\{k^*,n^*\}=\arg\max \Delta C_{k,n}$, until $\mathcal{N}_u=\emptyset$.

After subcarrier assignment, in the second step of SAR scheme, water-filling is carried out to assign the transmit power of each $D2D_k$ on its allocated subcarriers.

B. Ergodic Sum Capacity with Single Sub-cell Structure

Since both BSCR and SAR based sub-cell resource allocation are performed based on the CSI of K D2D pairs, which are i.i.d., the ergodic capacities of K D2D pairs are identical to each other. Therefore, the ergodic sum capacity of K D2D pairs can be obtained from (3), (4) and (9) as (13) shown at the bottom of this page, where the transmit power of assigned subcarrier n_k to $D2D_k$, P_{k,n_k}, is determined by the water-filling algorithm to allocate the maximum transmit power P_{max} to the set of assigned subcarriers $\mathcal{N}_k$ according to $\{h_{k,n_k}\}_{n_k\in\mathcal{N}_k}$. However, as the $\{h_{k,n_k}\}_{n_k\in\mathcal{N}_k}$ is determined by subcarrier assignment for a large K, thanks to the multi-user diversity, the power allocated to subcarrier n_k can be approximated by the power equally allocated to the set of subcarriers $\mathcal{N}_k$ [27], [28],

$$P_{k,n_k}\approx\frac{P_{max}}{N_k},\forall k\in\mathcal{K},\ n_k\in\mathcal{N}_k. \tag{14}$$

Considering that the transmit distance of any D2D pair is fixed to one and combining (13) and (14), we have

$$\bar{C}_{TOT}=KB\mathbb{E}_{\mathcal{N}_k,\{h_{k,n_k}\}_{n_k\in\mathcal{N}_k}}\left\{\sum_{n_k\in\mathcal{N}_k}\log_2\left(1+\frac{\xi|h_{k,n_k}|^2}{N_k}\right)\right\}, \tag{15}$$

where $\xi=\frac{P_{max}}{\sigma^2}$.

For BSCR scheme, each subcarrier is allocated to the D2D pair with the best CSI, therefore, full multi-user diversity of K D2D pairs can be achieved at each subcarrier assignment. As the square of magnitude of Rayleigh fading channel follows exponential distribution, according to order statistics of exponential distribution [29], the pdf of $|h_{k,n_k}|^2,\forall n_k\in\mathcal{N}_k$, can be obtained as

$$f_{|h_{k,n_k}|^2}(x)=K\cdot(1-e^{-x})^{K-1}\cdot e^{-x}. \tag{16}$$

Also, since the subcarrier assignment is determined by $\{h_{k,n}\}_{k\in\mathcal{K},n\in\mathcal{N}}$, which are i.i.d. for all the K D2D pairs and N subcarriers, each subcarrier is allocated to $D2D_k$ with equal probability $\frac{1}{K}$. Therefore, the number of allocated subcarriers to $D2D_k$, N_k, follows a binomial distribution with probability mass function (pmf) given by

$$\mathbb{P}_{BSCR}(N_k=n)=\binom{N}{n}\cdot\left(\frac{1}{K}\right)^n\cdot\left(1-\frac{1}{K}\right)^{N-n}, \tag{17}$$

where $\binom{N}{n}=\frac{N!}{n!\cdot(N-n)!}$ represents the binomial coefficient.

By taking (16) and (17) into (15), the ergodic sum capacity for BSCR scheme could be derived as

$$\bar{C}_{BSCR}=K\cdot B\cdot\sum_{n=1}^{N}n\cdot\int_0^\infty\log_2\left(1+\frac{\xi\cdot x}{n}\right)\cdot f_{|h_{k,n_k}|^2}(x)\,dx\cdot\mathbb{P}_{BSCR}(N_k=n). \tag{18}$$

For SAR scheme, the explicit distribution of $|h_{k,n_k}|^2$ and N_k are difficult to be obtained directly, since the subcarriers are assigned iteratively and each iteration is correlated with the preceding results. Although each subcarrier cannot be guaranteed to be assigned to the D2D pair with the best channel condition, (16) can be used to obtain an upper bound of the ergodic sum capacity by assuming full multi-user diversity of K D2D pairs. Moreover, Appendix A shows that when $\frac{N}{K}$ is large enough, the pdf of the relaxed continuous number of allocated subcarriers per D2D pair for SAR scheme, $\tilde{N}_k$, is fitted by

$$f_{\tilde{N}_k}^{SAR}\left(x;N,\frac{1}{K}\right)=\frac{x^{N-1}\cdot e^{-K\cdot x}\cdot K^N}{\Gamma(N)}, \tag{19}$$

where $\Gamma(N)=(N-1)!$, as N is a positive integer.

By taking (16) and (19) into (15), an upper bound of the ergodic sum capacity for SAR scheme can be obtained as

$$\bar{C}_{SAR}\le\bar{C}_{SAR}^u=KB\int_0^\infty\int_0^\infty y\cdot\log_2\left(1+\frac{\xi\cdot x}{y}\right)\cdot f_{|h_{k,n_k}|^2}(x)\,dx\cdot f_{\tilde{N}_k}^{SAR}(y)\,dy, \tag{20}$$

where the equality holds when $\frac{N}{K}\to\infty$.

Figs. 2(a)-(b) show the numerical and simulation results of ergodic sum capacity for both BSCR scheme and SAR scheme when the number of subcarriers N and the number of D2D pairs K vary, respectively. It can be clearly seen that the numerical results of (18) matches the simulation results for BSCR scheme. For SAR scheme, the simulation results approach the numerical results of (20) with a negligible difference by increasing N or reducing K. This indicates that the upper bound derived in (20) is tightened when $\frac{N}{K}$ tends to infinity.

The optimal ergodic sum capacity is also shown in Fig. 2(a) for comparison, which is obtained by exhaustive search among all the possible subcarrier assignments for all K D2D pairs and N subcarriers. It is clearly shown that SAR scheme can always achieve near optimal ergodic sum capacity while the

$$\bar{C}_{TOT}=\mathbb{E}_{\{\mathcal{N}_k\}_{k\in\mathcal{K}},\{h_{k,n_k}\}_{k\in\mathcal{K},n_k\in\mathcal{N}_k}}\left\{\sum_{k\in\mathcal{K}}C_k\right\}=K\cdot\mathbb{E}_{\mathcal{N}_k,\{h_{k,n_k}\}_{n_k\in\mathcal{N}_k}}\left\{\sum_{n_k\in\mathcal{N}_k}B\cdot\log_2\left(1+\frac{P_{k,n_k}{d_k}^{-\alpha}|h_{k,n_k}|^2}{\sigma^2}\right)\right\}, \tag{13}$$

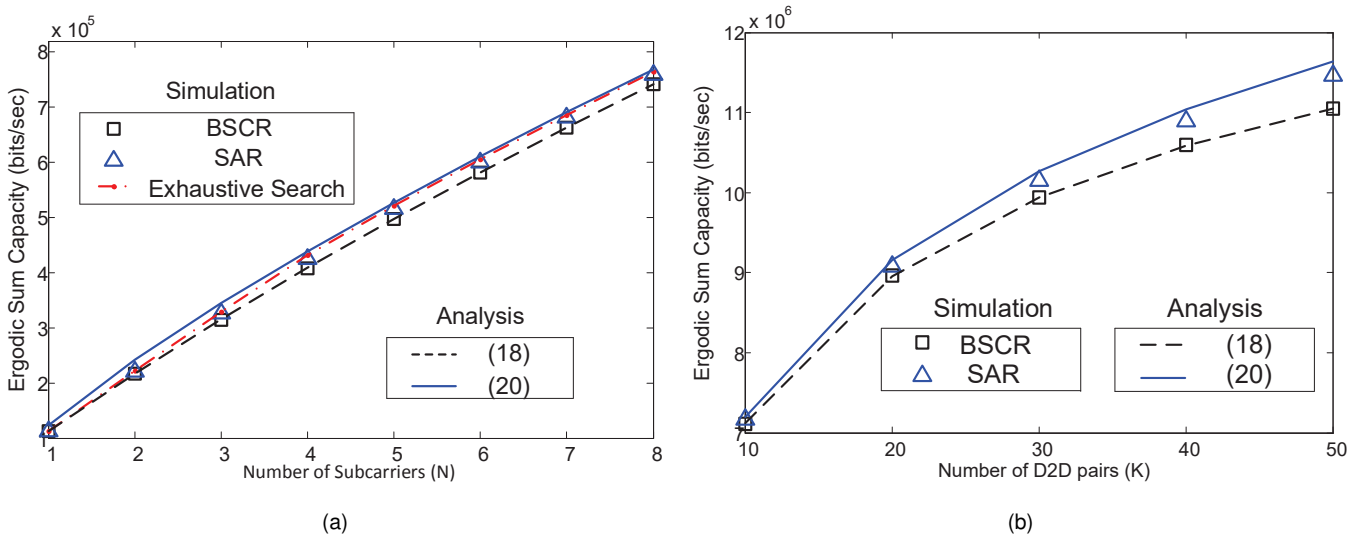

Fig. 2. Ergodic capacities for different resource allocation schemes versus a) the number of subcarriers N when $K = 4$ and b) the number of D2D pairs when $N = 100$, $\frac{P_{max}}{\sigma^2} = 100$ (20dB), $B = 15$KHz.

performance gap between the BSCR scheme and the optimal exhaustive search increases as N increases.

The closed form expressions of ergodic sum capacities with both SAR and BSCR schemes are further derived and summarized in Theorem 1 to show the performance difference between SAR and BSCR schemes. Specifically, the closed forms of (18) and (20) are obtained by using second order Taylor expansion to the channel gain and number of subcarriers per D2D pair, respectively.

Theorem 1. *The ergodic sum capacity of one cell with N subcarriers orthogonally assigned to K D2D pairs for BSCR-based resource allocation and SAR-based resource allocation can be approximated as*

$$\bar{C}_{BSCR} \approx B \cdot N \cdot \log_2\left(1 + \frac{\xi \cdot K \cdot \mathbb{H}(K)}{N}\right) - B \cdot (K-1) - \frac{B \cdot \pi^2 \cdot \xi^2}{12 \cdot \log(2) \cdot (\xi \cdot K \cdot \mathbb{H}(K) + N)^2}, \quad (21)$$

and

$$\bar{C}^u_{SAR} \approx \Omega(K, N, \xi), \quad (22)$$

respectively, where

$$\Omega(K, N, \xi) = \frac{B \cdot (N-1)^2}{N-2} \cdot \log_2\left(1 + \frac{\xi \cdot K \cdot \mathbb{H}(K)}{N-1}\right) - \frac{B \cdot \pi^2 \cdot (N-1) \cdot \xi^2 \cdot K^2}{12 \cdot \log 2 \cdot (\xi \cdot K \cdot \mathbb{H}(K) + N - 1)^2}, \quad (23)$$

$\mathbb{H}(K) = \sum_{k=1}^{K} \frac{1}{k}$ *is the harmonic number with its asymptotic limit* $\gamma + \log(K)$ *and* $\gamma \approx 0.5772156649$ *is the Euler-Mascheroni constant.*

Proof. See Appendix B □

The numerical results of (18) and (20)-(22), are presented in Fig. 3 with varying K and N. As we can clearly see from the figure, (21) and (22) serve as good approximations to

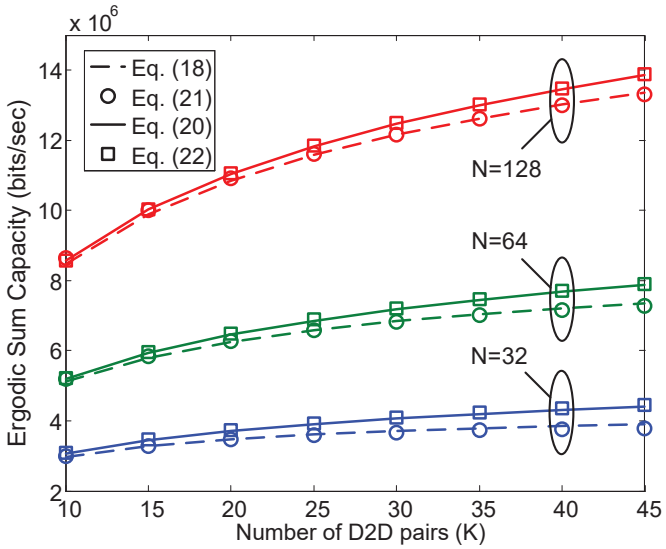

Fig. 3. Ergodic sum capacities for different resource allocation schemes versus the number of D2D pairs within the cell when $N = 32, 64, 128$, $\frac{P_{max}}{\sigma^2} = 100$ (20dB) and $B = 15$KHz.

(18) and (20), respectively, when either K or N scales. It is shown in (21) and (22) that $\bar{C}_{BSCR}$ scales in the order of $\Theta\left(N \log(\frac{K \log K}{N}) - K - \frac{1}{(K \log K + N)^2}\right)$ and $\tilde{C}_{SAR}$ scales in the order of $\Theta\left(N \log(\frac{K \log K}{N}) - \frac{NK^2}{(K \log K + N)^2}\right)$. Therefore, it can be concluded that the SAR scheme always achieves higher ergodic sum capacity than the BSCR scheme, especially when K is large.

IV. Sum Capacity under Multiple Sub-cell Structure

In contrast to the single sub-cell structure, the sum capacity of L sub-cells C_{TOT} is crucially affected by the inter D2D interference, as N subcarriers are universally reused among D2D

pairs within different sub-cells. Since the sub-cell resource allocation is performed in each sub-cell without any prior knowledge of inter D2D interference, the number of sub-cells L becomes a vital tuning parameter to adjust the inter D2D interference between different sub-cells. Particularly, as the inter D2D interference is determined by the positions of all the D2D pairs within the cell, in this section, the *average ergodic sum capacity* of L sub-cell structure over all possible D2D pair locations is investigated by delving into the formation of the inter D2D interference among different sub-cells, and the optimal number of sub-cells $\hat{L}_{opt}$ that can maximize the average ergodic sum capacity is discussed.

As mentioned in section II, the K D2D pairs are assumed to be distributed in the whole cell coverage according to a homogeneous PPP Φ_A with density λ_A. With the proposed sub-cell division strategy, the D2D pairs within each sub-cell l is then distributed as a PPP $\Phi_A^{(l)}$ with density $\lambda_A^{(l)} = \lambda_A$ and the number of D2D pairs in the sub-cell l, K_l, is Poisson distributed with pmf given by

$$\mathbb{P}(K_l = k) = \frac{\left(\pi \cdot {R_l}^2 \cdot \lambda_A^{(l)}\right)^k}{k!} e^{-\pi \cdot {R_l}^2 \cdot \lambda_A^{(l)}}. \tag{24}$$

For simplicity, let A_{k_l} be the location of $D2D_{k_l}$ with polar coordinates $(\gamma_{k_l}, \phi_{k_l})$, the average ergodic sum capacity $\bar{C}_{TOT}$ can be obtained from (7) as

$$\bar{C}_{TOT} = \mathbb{E}_{\Phi_A, \{h_{k,k',n}\}_{k\in\mathcal{K}, k'\in\mathcal{K}, n\in\mathcal{N}}} \left(\sum_{l=1}^{L} C_l \right), \tag{25}$$

where C_l is the sum capacity of sub-cell l, given by

$$C_l = \sum_{A_{k_l} \in \Phi_A^{(l)}} \sum_{n\in\mathcal{N}_{k_l}} B \cdot \log_2 \left(1 + \frac{P_{k_l,n} \cdot |g_{k_l,n}|^2}{I_{k_l,n}^c + \sigma^2} \right), \tag{26}$$

where $g_{k_l,n} = h_{k_l,n}$, as the transmit distance of $D2D_k$ is considered to be one.

Note that under PPP assumption, there are occasions when a sub-cell has no active D2D pair. Here, we denote active as the event of one sub-cell having at least one D2D pair within its coverage, which has the probability

$$\mathbb{P}(\text{active}) = 1 - \mathbb{P}(K_l = 0) = 1 - e^{-\pi \cdot {R_l}^2 \cdot \lambda_A^{(l)}}. \tag{27}$$

Let $\mathcal{L}_{active}$ denote the active sub-cell set, which contains sub-cells having at least one D2D pair, with $|\mathcal{L}_{active}| = L_{active}$. Since the cell is geographic symmetrically divided into L sub-cells, the pmf of the number of active sub-cells, L_{active}, can be obtained as

$$\mathbb{P}(L_{active} = l) = \binom{L}{l} \left(1 - e^{-\pi \cdot {R_l}^2 \cdot \lambda_A^{(l)}}\right)^l \left(e^{-\pi \cdot {R_l}^2 \cdot \lambda_A^{(l)}}\right)^{L-l}. \tag{28}$$

For the purpose of illustration, the central sub-cell is assumed as the reference sub-cell l_r, and one typical D2D pair randomly located at $A_{k_r}(\gamma_{k_r}, \phi_{k_r})$ within sub-cell l_r is assumed as the reference D2D pair $D2D_{k_r}$. By combining (25) and (28), the average ergodic sum capacity can be rewritten as[3]

$$\bar{C}_{TOT} = \sum_{l=1}^{L} l \cdot \mathbb{P}(L_{active} = l) \cdot \bar{C}_r, \tag{29}$$

where $\bar{C}_r$ is the average sum capacity of active sub-cell l_r, given by

$$\bar{C}_r = \mathbb{E}_{\Phi_A, \{h_{k_r,k',n}\}_{k'\in\mathcal{K}, n\in\mathcal{N}_{k_r}}} \left[\sum_{A_{k_r} \in \Phi_A^{(r)}} \sum_{n\in\mathcal{N}_{k_r}} B \cdot \log_2 \left(1 + \frac{P_{k_r,n} |h_{k_r,n}|^2}{I_{k_r,n}^c + \sigma^2} \right) \right]. \tag{30}$$

According to the sub-cell resource allocation, if one sub-carrier is allocated to $D2D_{k_r}$, there must be one D2D pair $D2D_{k_{l'}}$ in each active sub-cell in $\mathcal{L}_{active}$ except l_r that reuses the same subcarrier, and thus introduces inter D2D interference to $D2D_{k_r}$. That is, there exist $L_{active} - 1$ inter D2D interference signals on each subcarrier $n \in \mathcal{N}_{k_r}$ allocated to $D2D_{k_r}$.

By performing sub-cell resource allocation independently in each active sub-cell, the inter D2D interference signal on any allocated subcarrier $n \in \mathcal{N}_{k_r}$ received at $D2D_{k_r}$ from sub-cell $l' \in \mathcal{L}_{active} \setminus \{l_r\}$ follows the same distribution, as the D2D pairs are randomly distributed and the small scale fading on each subcarrier follows an independent and identical Rayleigh distribution. Hence, the cumulative inter D2D interference received at $D2D_{k_r}$ on each allocated subcarrier $n \in \mathcal{N}_{k_r}$ has the same distribution as well. Therefore, the inter D2D interference in this section is specified for one subcarrier $n_r \in \mathcal{N}_{k_r}$. It is shown in [30] that in a dense D2D deployed system, the cumulative inter D2D interference signal can be modelled as a complex Gaussian random variable with zero mean and variance I_{k_r,n_r}^v. Then, we have

$$I_{k_r,n_r}^c \approx I_{k_r,n_r}^v = \sum_{l'\in\mathcal{L}_{active}\setminus\{l_r\}} P_{k_{l'},n_r} \cdot {d_{k_r,k_{l'}}}^{-\alpha}, \tag{31}$$

where $P_{k_{l'},n_r}$ is the transmit power of $D2D_{k_{l'}}$ on subcarrier n_r and $d_{k_r,k_{l'}}$ is the distance between $D2D_{k_{l'}}$ and $D2D_{k_r}$. As the interference power I_{k_r,n_r}^v is a function of $P_{k_{l'},n_r}$ and $d_{k_r,k_{l'}}$, let us first study them, respectively.

a) Transmit power on subcarrier n_r, P_{k_l,n_r} : Similar to the single sub-cell structure, P_{k_l,n_r} can be approximated by the average power of $D2D_{k_l}$ over allocated subcarriers as

$$P_{k_l,n_r} \approx \frac{P_{max}}{N_{k_l}}, \tag{32}$$

where N_{k_l} is the number of allocated subcarriers to $D2D_{k_l}$, which is determined by the single sub-cell resource allocation scheme. Since SAR scheme achieves near optimal ergodic sum

[3]Since a single cell is adjacent to multiple cells in practical systems, any sub-cell could be surrounded by multiple sub-cells, which is similar to the reference sub-cell. Hence, without loss of generality, it is assumed that each active sub-cell has the same average ergodic sum capacity as the reference sub-cell.

$$F_{d_{k_r,k_{l'}}|\gamma_{k_r}}(x|y)=\begin{cases}\frac{x^2\arccos\frac{R_l^2-x^2-y^2}{2xy}-R_l^2\arccos\frac{R_l^2+y^2-x^2}{2R_ly}+2M(R_l)}{\pi(R^2-R_l^2)} & R_l-y<x\le R_l+y\\ \frac{x^2-R_l^2}{R^2-R_l^2} & R_l+y<x\le R-y\\ \frac{x^2\arccos\frac{x^2+y^2-R^2}{2xy}+R^2\arccos\frac{R^2+y^2-x^2}{2Ry}-2M(R)-\pi R_l^2}{\pi(R^2-R_l^2)} & R-y<x\le R+y\end{cases}, \tag{34}$$

$$\bar{C}_r=\sum_{k=1}^{\infty}k\cdot\mathbb{P}(K_r=k|\text{active})\int_0^N n\cdot f_{N_{k_r}}(n)\int_0^{\infty}f_{|h_{k_r,n}|^2}(h)\int_0^{R_l}f_{\gamma_{k_r}}(d_r)\cdot\Bigg[\sum_{l'\in\mathcal{L}_{active}\setminus\{l_r\}}\sum_{k'=1}^{\infty}\mathbb{P}(K_{l'}=k'|\text{active})$$
$$\int\cdots\int_{2(L_{active}-1)}C_s\prod_{l'\in\mathcal{L}_{active}\setminus\{l_r\}}f_{N_{k_{l'}}}(n_{l'})\,dn_{l'}\cdot f_{d_{k_r,k_{l'}}|\gamma_{k_r}}(d_{l'}|d_r)\mathrm{d}d_{l'}\Bigg]\,dd_r\,dh\,dn, \tag{37}$$

capacity in single sub-cell structure, as shown in Section III-B, it is assumed that SAR scheme is adopted by each active sub-cell under L sub-cell structure.[4]

Note that the pdf of N_{k_l} is given by (19), which is a function of the number of D2D pairs K_l within the active sub-cell l. The conditional pmf of K_l can be further derived from (24) and (27) as

$$\mathbb{P}(K_l=k|\text{active})=\frac{\left(\frac{\bar{K}}{L}\right)^k\cdot e^{-\frac{\bar{K}}{L}}}{k!}\cdot\frac{1}{1-e^{-\frac{\bar{K}}{L}}}. \tag{33}$$

b) Interference distance, $d_{k_r,k_{l'}}$: Since the locations of the interfering D2D pairs are random, it is assumed that $L_{active}-1$ interfering D2D pairs of $D2D_{k_r}$ are uniformly distributed over the cell except sub-cell l_r. Appendix C shows that conditioned on the location of $D2D_{k_r}$, $A_{k_r}(\gamma_{k_r},\phi_{k_r})$, the cumulative distribution function (cdf) of $d_{k_r,k_{l'}}$, $F_{d_{k_r,k_{l'}}|\gamma_{k_r}}(x|y)$, is given by (34) shown at the top of this page, where

$$M(r)=\sqrt{\tfrac{r+x+y}{2}\left(\tfrac{r+x+y}{2}-r\right)\left(\tfrac{r+x+y}{2}-x\right)\left(\tfrac{r+x+y}{2}-y\right)}, \tag{35}$$

and γ_{k_r} is the distance between $D2D_{k_r}$ and the centre of the cell with the pdf

$$f_{\gamma_{k_r}}(x)=\frac{2x}{R_l^2},\qquad 0\le x\le R_l. \tag{36}$$

By substituting (31) and (32) into (30), the average ergodic sum capacity of the reference sub-cell can be expressed as (37), where

$$C_s=B\cdot\log_2\left(1+\frac{P_{max}h}{n\left(\sum_{l'\in\mathcal{L}_{active}\setminus\{l_r\}}\frac{P_{max}}{n_{l'}}{d_{l'}}^{-\alpha}+\sigma^2\right)}\right). \tag{38}$$

It is seen in (37) that multi-fold integral operation is required to obtain the numerical results of (29), as the cumulative property of inter D2D interference leads to $3\cdot(L_{active}-1)$ random variables. Therefore, we will further simplify the cumulative inter D2D interference model in the following in order to obtain a tractable analytical expression of (37).

Note that the transmit power $P_{k_{l'},n_r}$ in (31) is i.i.d., the cumulative inter D2D interference for $D2D_{k_r}$ can be greatly simplified as

$$I^v_{k_r,n_r}\approxeq\tilde{I}^v_{k_r,n_r}=\frac{P_{max}}{\mathbb{E}\left[N_{k_{l'}}\right]}\cdot\sum_{l'\in\mathcal{L}_{active}\setminus\{l_r\}}{d_{k_r,k_{l'}}}^{-\alpha}, \tag{39}$$

where the equality holds when $\frac{L}{K}\to\infty$, i.e., each D2D pair reuses N subcarriers universally. As (34) is a piecewise function with complicated sub-domain functions, (39) is difficult to be tackled. Fortunately, it can be easily observed that when $D2D_{k_r}$ located at the central of the l_r, i.e. $\gamma_{k_r}=0$, the sub-domain of first and third sub-functions of $F_{d_{k_r,k_{l'}}}$ are empty. Thus, (34) can be simplified as

$$F_{d_{k_r,k_{l'}}|\gamma_{k_r}=0}(x)=\frac{x^2-R_l^2}{R^2-R_l^2},\qquad R_l<x<R. \tag{40}$$

According to (4) and (40), the pdf of path loss, ${d_{k_r,k_{l'}}}^{-\alpha}$, can be obtained as

$$f_{{d_{k_r,k_{l'}}}^{-\alpha}|\gamma_{k_r}=0}(x)=\frac{2\cdot x^{-\frac{2}{\alpha}-1}}{\alpha\cdot(R^2-R_l^2)},\qquad R^{-\alpha}<x<R_l^{-\alpha}, \tag{41}$$

which indicates that ${d_{k_r,k_{l'}}}^{-\alpha}$ is a bounded Pareto-distributed random variable when $\gamma_{k_r}=0$.

Theorem 2. *Let $Y=\sum_{n=1}^{N}X_n$, $X_{max}=\max\{X_1,\cdots,X_N\}$ and $r=\frac{Y}{X_{max}}$. If $X_1,\cdots,X_n$ follow i.i.d. bounded Pareto distribution with*

$$f(x)=\frac{\beta\cdot x^{-1-\beta}}{1-c^{-\beta}},\quad 1<x<c,\quad \beta>0, \tag{42}$$

then

$$\mathbb{E}\left[r\right]=\frac{1}{1-\beta}+N\left[1-\frac{1}{1-c^{-\beta}}+\frac{1}{1-\beta}\left(\frac{c^{-\beta}-\beta c^{-1}}{1-c^{-\beta}}-\frac{B_{inc}(1-c^{-\beta},N,\frac{1}{\beta})}{(1-c^{-\beta})^N}\right)\right], \tag{43}$$

[4]Note that although SAR scheme is assumed in this section due to its superior performance, the analysis can be applied to any sub-cell resource allocation scheme in the same manner.

$$\Psi(\alpha,u,L_{active})=\mathbb{E}\left(\frac{\sum_{l'\in\mathcal{L}_{active}\setminus\{l_r\}} {d_{k_r,k_{l'}}}^{-\alpha}}{{d_{k_r}^*}^{-\alpha}}\right)$$
$$=\frac{\alpha}{\alpha-2}+(L_{active}-1)\left[1-\frac{1}{1-u^2}+\frac{\alpha}{\alpha-2}\left(\frac{u^2-\frac{2}{\alpha}u^\alpha}{1-u^2}-\frac{B_{inc}(1-u^2,L_{active}-1,\frac{\alpha}{2})}{(1-u^2)^{(L_{active}-1)}}\right)\right], \quad (45)$$

$$\bar{C}^u_{TOT}=B\cdot\sum_{l=1}^{L}l\cdot\mathbb{P}(L_{active}=l)\cdot\sum_{k_r=1}^{\infty}k_r\cdot\mathbb{P}(K_r=k_r|\text{active})\cdot\int_0^N n\cdot f_{N_{k_r}}(n)\cdot\int_0^\infty f_{|h_{k_r,n}|^2}(h)$$
$$\int_{R_l}^{R}f_{d^*_{k_r}|(\gamma_{k_r}=0)}(x)\cdot\log_2\left(1+\frac{P_{max}\cdot h}{n\cdot\left(\frac{P_{max}}{\mathbb{E}\left[N_{k_{l'}}\right]}\cdot\Psi(\alpha,u,l)\cdot x^{-\alpha}+\sigma^2\right)}\right)dx\,dh\,dn. \quad (47)$$

where $B_{inc}(x,y,z)=\int_0^x t^{y-1}(1-t)^{z-1}\,dt$ is the incomplete beta-function.

Proof. See Appendix D. □

Remark. *Intuitively, due to the heavy-tailed property of bounded Pareto distribution, the summation of N i.i.d. bounded Pareto random variables, Y, is closely related to the largest value among N random variables, X_{max}. According to Theorem 2, Y can be approximated as $\mathbb{E}\{\frac{Y}{X_{max}}\}X_{max}$, where $\mathbb{E}\{\frac{Y}{X_{max}}\}$ is derived as a function of N, the shape parameter β and the location parameter c of the bounded Pareto distribution.*

Since ${d_{k_r,k_{l'}}}^{-\alpha}$ is a bounded Pareto-distributed random variable when $\gamma_{k_r}=0$, the summation of $L_{active}-1$ i.i.d. Pareto random variables in (39) can be simplified. Specifically, the conditional cumulative interference received at $D2D_{k_r}$, when $\gamma_{k_r}=0$, can be approximated as

$$\tilde{I}^v_{k_r,n_r|\{\gamma_{k_r}=0\}}\approx\frac{P_{max}}{\mathbb{E}\left[N_{k_{l'}}\right]}\cdot\Psi(\alpha,u,L_{active})\cdot{d^*_{k_r}}^{-\alpha}, \quad (44)$$

where $d^*_{k_r}=\min_{l'\in\mathcal{L}_{active}\setminus\{l\}}d_{k_r,k_{l'}}$ denotes the smallest distance among the distances of $L_{active}-1$ inter D2D interference and $\Psi(\alpha,u,L_{active})$ can be seen as the offset parameter, which is shown in (45) at the top of this page, with $u=\frac{R_l}{R}=\left(\frac{3}{4L-1}\right)^{-\frac{1}{2}}$. Finally, the pdf of $d^*_{k_r}$ is obtained according to the order statistics theory [29], as

$$f_{d^*_{k_r}|L_{active}}(x|l)=(l-1)\left(1-F_{d_{k_r,k_{l'}}}(x)\right)^{l-2}f_{d_{k_r,k_{l'}}}(x),$$
$$R_l\le x\le R. \quad (46)$$

(44) reveals that the cumulative interference received at $D2D_{k_r}$ is related to the closest interference D2D pair. Intuitively, as the interference signal strength exponentially decreases with the interfering distance, the nearest interferer contributes the most to the received interference.

For $0<\gamma_{k_r}\le R_l$, due to the growing dominant effect of $d^*_{k_r}$ on the cumulative interference received at $D2D_{k_r}$, $I^v_{k_r,n_r}$, the average cumulative interference $\mathbb{E}\left[I^v_{k_r,n_r}\right]$ is a monotonic increasing function of γ_{k_r} from $\mathbb{E}\left[I^v_{k_r,n_r|\{\gamma_{k_r}=0\}}\right]$ to $\mathbb{E}\left[I^v_{k_r|\{\gamma_{k_r}=R_l\}}\right]$. Moreover, it can be easily observed that $\mathbb{E}\left[I^v_{k_r|\{\gamma_{k_r}=R_l\}}\right]=\infty$, since $\mathbb{E}\left[{d^*_{k_r}}^{-\alpha}\right]=\infty$ when $\gamma_{k_r}=R_l$. Therefore, an upper bound of the $\bar{C}_{TOT}$ can be obtained by using $\tilde{I}^v_{k_r|\{\gamma_{k_r}=0\}}$ in (44) as a lower bound of the cumulative interference.

The upper bound of the $\bar{C}_{TOT}$ is shown in (47) at the top of this page, by substituting (30) and (44) into (29). Since the sub-cell resource allocation is independent with each other and the fading channels among D2D pairs are i.i.d., the integrations and summations in (47) can be interchanged, and $\bar{C}^u_{TOT}$ can be further simplified according to Theorem 1 as,

$$\bar{C}^u_{TOT}=\sum_{l=1}^{L}l\cdot\mathbb{P}(L_{active}=l)\sum_{k_r=1}^{\infty}\mathbb{P}(K_r=k_r|\text{active})\int_{R_l}^{R}$$
$$f_{d^*_{k_r}|(\gamma_{k_r}=0)}(x)\Omega(k_r,N,\xi_I(x,\mathbb{E}\left[N_{k_{l'}}\right]))\,dx \quad (48)$$

where $\xi_I(x,\mathbb{E}\left[N_{k_{l'}}\right])=\frac{P_{max}}{\Psi(\alpha,u,l)\cdot P_{max}\cdot x^{-\alpha}/\mathbb{E}\left[N_{k_{l'}}\right]+\sigma^2}$ and $\mathbb{E}\left[N_{k_{l'}}\right]=\frac{N}{K_{l'}}$ according to (19).

Fig. 4(a) shows the simulation results of average ergodic sum capacity of the cell under L sub-cell structure vary with the average number of D2D pairs $\bar{K}$. Also, the numerical results of the upperbound $\bar{C}^u_{TOT}$ shown in (48) are plotted. Note that as the average number of D2D pairs $\bar{K}$ increases, the total transmit power within the cell increases linearly, since each D2D pair has the same individual transmit power P_{max}. Due to the combined effect of the multi-user diversity and the total transmit power, the average ergodic sum capacity of the cell under L sub-cell structure increases as $\bar{K}$ increases. Moreover, it can be clearly seen in Fig. 4(a) that the increasing slopes of average ergodic sum capacities for different L structures are not the same. For instance, the capacity gap between $L=7$ and $L=19$ increases when $\bar{K}$ increases. A cross point is shown between $L=19$ and $L=37$ at $\bar{K}=28$, which indicates that when $\bar{K}<28$, the average ergodic sum capacity of the system under $L=19$ structure is larger than that under $L=37$. This phenomenon is caused by the effects of subcarriers being spatially reused among active sub-cells and the accompanied cumulative inter D2D interference. Specifically, when L increases, the number of

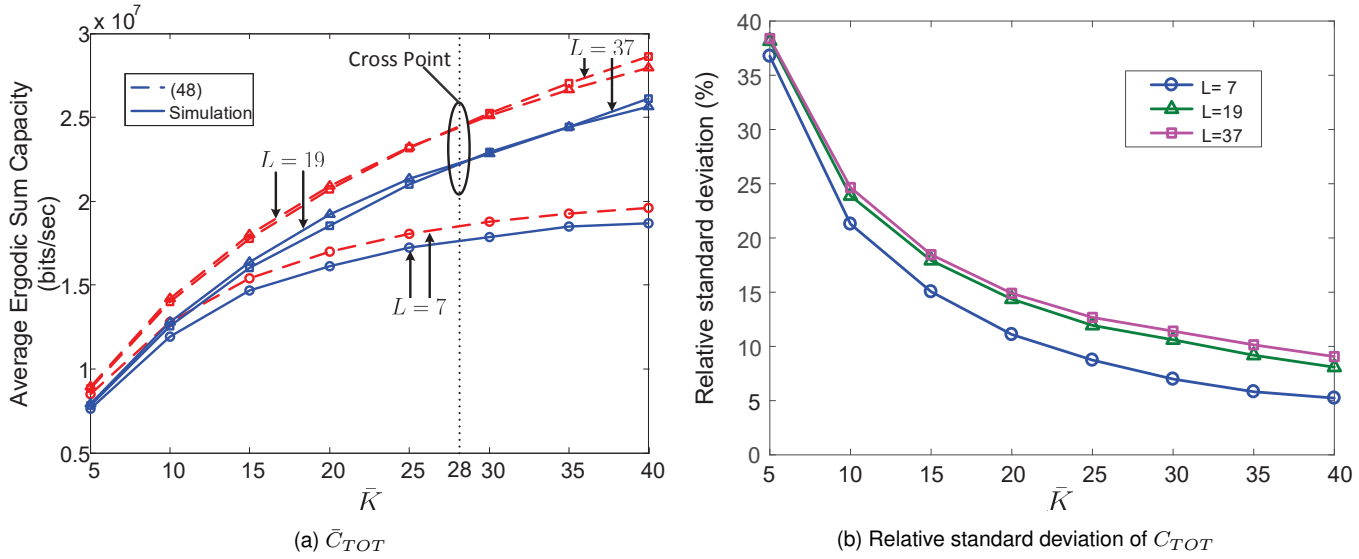

(a) $\bar{C}_{TOT}$ (b) Relative standard deviation of C_{TOT}

Fig. 4. (a) Average ergodic sum capacity and (b) relative standard deviation of sum capacity versus $\bar{K}$ under 10^4 random realizations of D2D pairs following a PPP, when $L = 7, 19, 37$. $B = 15$KHz, $R = 10$, $\frac{P_{max}}{\sigma^2} = 1000$ (30dB), $N = 32$ and $\alpha = 3$.

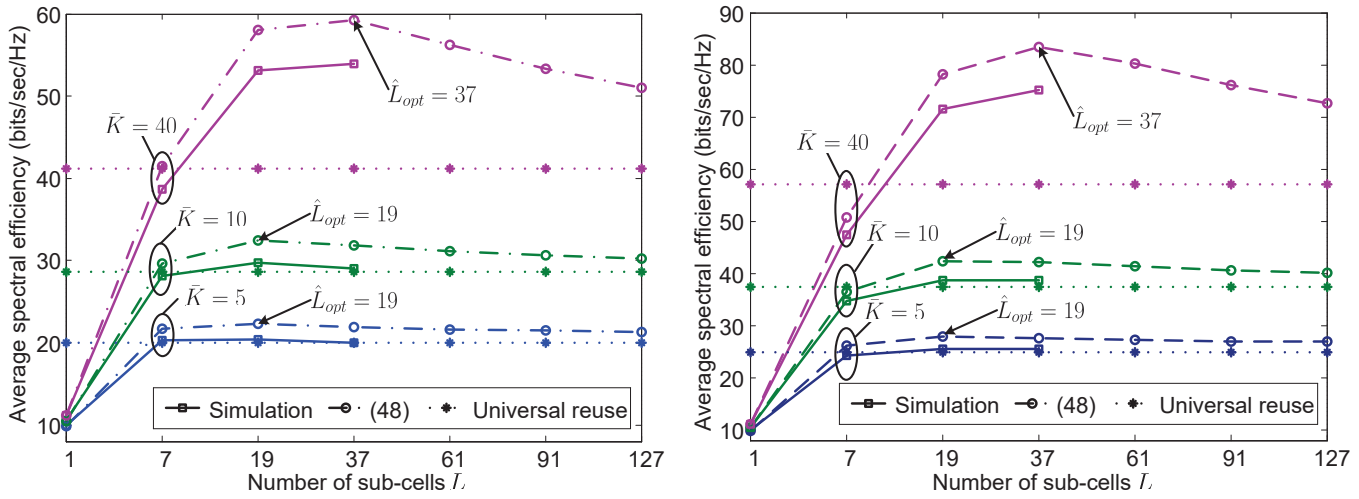

(a) $\alpha = 3$ (b) $\alpha = 4$

Fig. 5. Spectral efficiency versus the number of subcells under 10^4 random realizations of D2D pairs following a PPP, when a) $\alpha = 3$ and b) $\alpha = 4$. $B = 15$KHz, $R = 10$, $\frac{P_{max}}{\sigma^2} = 1000$ (30dB), $\frac{N}{K} = 1$.

active sub-cells, L_{active} increases according to (28). As N subcarriers are reused among active sub-cells, the frequency reuse factor increases as L_{active} increases, whereas in the mean time, average ergodic sum capacity is strongly limited by the cumulative inter D2D interference, which is a function of L_{active}, as shown in (44). Therefore, there exists an optimal number of sub-cells $\hat{L}_{opt}$, which can maximize the average ergodic sum capacity of our proposed resource allocation framework. Moreover, as the cross point of $\bar{C}^u_{TOT}$ matches the simulation result in Fig. 4(a), (48) can be used to characterise the average system sum capacity under different L structure.

The relative standard deviation of sum capacity, which is the ratio of the standard deviation of the sum capacity to the average ergodic sum capacity, under 10^4 random realizations of D2D pairs following a PPP is shown in Fig. 4(b). We can clearly see that the relative standard deviation of sum capacity under $L = 7, 19, 37$ sub-cell structures monotonically decreases as the average number of D2D pairs increases, and finally approaches to less than 10% when $\bar{K} = 40$. This indicates that the variance of the sum capacity is very small in dense D2D deployed scenarios. Hence, the system performance could be well presented by the average ergodic sum capacity and the optimal number of sub-cells $\hat{L}_{opt}$ could be used to maximize the sum capacity effectively, especially in dense D2D deployed scenarios.

For a better view of the optimal number of sub-cells, $\hat{L}_{opt}$, Figs. 5(a) and 5(b) present the average spectral efficiency, which is the average ergodic sum capacity normalized by $N \cdot B$, as a function of the number of sub-cells. The upper bound of the average spectral efficiency, $\frac{\bar{C}^u_{TOT}}{N \cdot B}$, is also shown

in Figs. 5(a) and 5(b). To eliminate the effect of total transmit power on the average spectral efficiency, the number of subcarriers N is set to be the same as $\bar{K}$.

Since the CSI of interference channels between D2D pairs is not available at the BS, the subcarriers are either orthogonally assigned to all D2D pairs in the cell (referred to as orthogonal scheme) or fully reused by all the D2D pairs in the cell (referred to as universal reuse scheme) apart from our proposed D2D sub-cell division strategy. The average spectral efficiencies of both schemes are shown in Figs. 5(a)-(b) as the benchmarks of our proposed sub-cell division based resource allocation framework. Note that the orthogonal resource allocation is equivalent to the single sub-cell scenario in our proposed framework, and the numerical results of average spectral efficiency can be obtained via (22). It can be seen from Fig. 5 that the average spectral efficiency improves dramatically when L increases from one and then decreases after reaching a certain value. This is consistent with the conclusion drawn from Fig. 4(a) and the analysis that there exists an optimal number of sub-cells $\hat{L}_{opt}$ to maximize the average spectral efficiency. Further, the average spectral efficiency converges to the universal reuse results as L goes to infinity. The reason is that as L increases unboundedly, L_{active} finally converges to the number of D2D pairs. Furthermore, it is noticed that the gap between the optimal point to the universal reuse result increases significantly as $\bar{K}$ increases, which reveals that the average spectral efficiency can be greatly improved with $\hat{L}_{opt}$ obtained via (48) by adopting the proposed resource allocation framework in dense D2D deployed scenarios (e.g. $\bar{K} \geq 10$). For sparse D2D scenarios (e.g. $\bar{K} < 10$), $\hat{L}_{opt}$ can be approximated to 7 as the gap between the maximum spectral efficiency and that with $L = 7$ is negligible.

V. Conclusion

In this paper, the resource allocation for cellular D2D underlaid OFDMA systems has been studied to maximize the average ergodic sum capacity. By taking advantage of the spatial dispersion nature of D2D pairs, a simple, yet effective resource allocation framework was proposed with significantly reduced CSI feedback signalling overhead compared to existing schemes. The theoretical analysis of system sum capacity was then performed through in-depth study of cumulative inter D2D interference. A tractable analytical expression of the average ergodic sum capacity was derived and further used to obtain the optimal number of D2D pair groups. It was demonstrated that with small CSI feedback, substantial capacity gains can be achieved by cellular D2D communications with the proposed resource allocation framework. It was also suggested that when the number of D2D pairs in the cell is small (e.g. less than 10), dividing the whole cell into seven sub-cells is enough to obtain near optimal spectral efficiency.

Note that a geography-based sub-cell division strategy was proposed in this paper to group D2D pairs according to their location information, which was assumed to be perfectly known at the BS. In practical systems, however, the location information could be inaccurate. It is therefore important to study the impact of location information error on the performance of our proposed resource allocation framework in future studies. Also, this paper aimed at maximizing the average ergodic sum capacity of D2D pairs from the system's perspective. How to further ensure fairness among D2D pairs deserves much attention in future work.

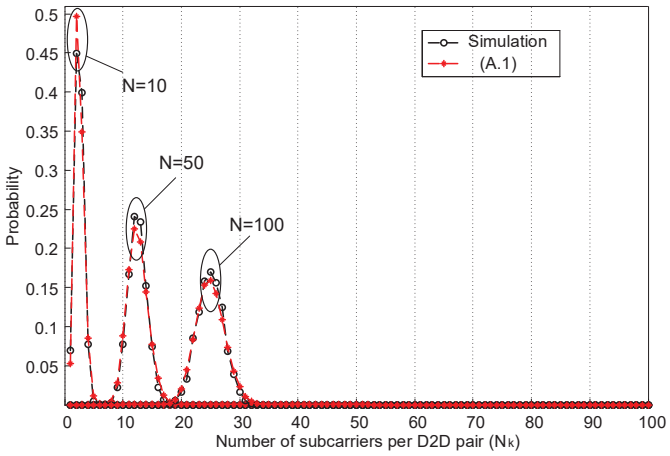

Fig. 6. Probability of the number of allocated subcarriers per D2D pair when $\frac{P_{max}}{\sigma^2} = 100$ (20dB) , $K = 4$

Appendix A
Validation of (19)

Since the small-scale channel fading factors are i.i.d. for all K D2D pairs, the mean value of the number of subcarriers allocated to $D2D_k$, N_k, is $\frac{N}{K}$. As N_k is a discrete value, it is difficult to obtain the explicit probability mass function (pmf). By relaxing N_k into a continuous variable $\tilde{N}_k$, the gamma distribution can be used to approximate the pdf of N_k, with the shape parameter approximated by N and the rate parameter approximated by K. The corresponding pdf of $\tilde{N}_k$ is then given by

$$f_{\tilde{N}_k}^{SAR}(x; N, \frac{1}{K}) = \frac{x^{N-1} \cdot e^{-K \cdot x} \cdot K^N}{\Gamma(N)}. \qquad \text{(A.1)}$$

In order to show the accuracy of the approximation, the pmf of N_k under 10^5 subcarrier assignment results with SAR-based resource allocation scheme is shown in Fig. 6, compared with the numerical result of (A.1). It can be seen that given the number of D2D pairs $K = 4$, when the total number of subcarriers is relatively large, e.g. larger than 40, the approximated Gamma distribution for $\tilde{N}_k$ is very close to the practical simulation results of N_k. This is due to the fact that gamma function is continuous while N_k is a positive integer. Hence, it is clear that the approximation becomes more accurate as $\frac{N}{K}$ enlarges.

Appendix B
Proof of Theorem 1

From the pdf of the best subchannel's channel fading factor $|h_{k,n_k}|^2$ in (16), the mean and variance of $|h_{k,n_k}|^2$ can be

$$\bar{C}_{BSCR} = BN\log_2\left(1+\frac{\xi K\mathbb{H}(K)}{N}\right) - \frac{B\pi^2\xi^2}{12\log(2)\cdot(\xi\cdot K\mathbb{H}(K)+N)^2} - B(K-1)\underbrace{\frac{b^4+2N(1-c)b^3+N^2(1+c)b^2}{(b+N)^4}}_{\Delta}, \tag{B.9}$$

derived as

$$\begin{aligned}\mu_{h^*} &= \int_0^\infty x\cdot K\cdot\left(1-\exp^{-x}\right)^{K-1}\cdot\exp^{-x}\,dx \\ &= \mathbb{H}(K) \overset{K\to\infty}{\sim} \log(K),\end{aligned} \tag{B.1}$$

and

$$\begin{aligned}\sigma^2_{h^*} &= \int_0^\infty x^2\cdot K\cdot\left(1-\exp^{-x}\right)^{K-1}\cdot\exp^{-x}\,dx - \mathbb{H}(K)^2 \\ &= \frac{\pi^2}{6} - \psi^{(1)}(1+K) \overset{K\to\infty}{\sim} \frac{\pi^2}{6},\end{aligned} \tag{B.2}$$

respectively, where $\mathbb{H}(K)=\sum_{k=1}^{K}\frac{1}{k}$ is the harmonic number with its asymptotic limit $\gamma+\log(K)$ and $\gamma\approx 0.5772156649$ is the Euler-Mascheroni constant. $\psi^{(1)}(z)$ is the polygamma function of order 1. According to Taylor's theory, the analytic function of (15) centred at $\bar{C}_{TOT}(\mu_{h^*})$ is shown as

$$\bar{C}_{TOT} = K\cdot B\cdot\mathbb{E}_{\mathcal{N}_k,\{h_{k,n_k}\}_{n_k\in\mathcal{N}_k}}\left\{\sum_{n_k\in\mathcal{N}_k}\sum_{m=0}^{\infty}\frac{g^{(m)}(\mu_{h^*})}{m!}\cdot\left(|h_{k,n_k}|^2-\mu_{h^*}\right)^m\right\}, \tag{B.3}$$

where $g^{(m)}(x)$ denotes the mth derivative of $g(x)$, and

$$g(x) = \log_2\left(1+\frac{\xi\cdot x}{N_k}\right). \tag{B.4}$$

Based on the pdf of $|h_{k,n_k}|^2$ given by (20), the pdf of $g(|h_{k,n_k}|^2)$ can be expressed as

$$f_{g(|h_{k,n_k}|^2)}(x) = \frac{K\log 2\cdot 2^y\cdot e^{\frac{N_k(1-2^y)}{\xi}}\left(1-e^{\frac{N_k(1-2^y)}{\xi}}\right)^{K-1}}{\frac{\xi}{N_k}}\cdot q(x) \tag{B.5}$$

From Fig. 7, it can be seen that the pdf of $g(|h_{k,n_k}|^2)$ is approximately symmetrically centred at $g(\mu_{h^*})$. Thus, (B.3) can be approximated by the second-order Taylor's polynomial, which is

$$\bar{C}_{TOT} \approx K\cdot B\cdot\mathbb{E}_{N_k}\left\{N_k\cdot\left[\log_2\left(1+\frac{\xi\cdot\mu_{h^*}}{N_k}\right)-\sigma^2_{h^*}\cdot\left(\frac{\xi^2}{2\log(2)\cdot {N_k}^2\cdot\left(1+\frac{\xi\cdot\mu_{h^*}}{N_k}\right)^2}\right)\right]\right\}. \tag{B.6}$$

Similarly, as the pmf of N_k for BSCR-based sub-cell resource allocation schemes given in (17) is a symmetric function, $\bar{C}_{TOT}$ can be approximated by the second-order Taylor's polynomial centred at $\bar{C}_{TOT}(\mathbb{E}[N_k])$. The ergodic capacity for BSCR-based sub-cell resource allocation scheme can be shown as

$$\bar{C}_{BSCR} \approx K\cdot B\cdot\left(q(\mu_{N_k})+\frac{q^{(2)}(\mu_{N_k})\cdot\sigma^2_{N_k}}{2}\right), \tag{B.7}$$

where $\mu_{N_k}=\frac{N}{K}, \sigma^2_{N_k}=\frac{N(K-1)}{K^2}$ and

$$q(x) = x\left[\log_2\left(1+\frac{\xi\mu_{h^*}}{x}\right)-\left(\frac{\xi^2}{2x^2\left(1+\frac{\xi\mu_{h^*}}{x}\right)^2\log(2)}\right)\sigma^2_{h^*}\right]. \tag{B.8}$$

After some manipulation, the closed form of $\bar{C}_{BSCR}$ can be expressed as (B.9) shown at th top of this page, where $b=\xi\cdot K\cdot\mathbb{H}(K)$ and $c=\frac{\pi^2}{6\mathbb{H}(K)^2}$. Since $b\geq 1$ and it is monotonically increasing with K, we have $\Delta\approx 1$. Thus, the last term of (B.9) can be approximated to $B\cdot(K-1)$ and (21) can be obtained.

For SAR resource allocation scheme, since $\tilde{N}_k$ follows Gamma distribution, the reciprocal random variable $a=\frac{1}{\tilde{N}_k}$ follows inverse gamma distribution with $\mu_a=\frac{K}{N-1}$ and $\sigma^2_a=\frac{K^2}{(N-1)^2\cdot(N-2)}$. $\bar{C}^u_{SAR}$ can be then approximated by the second-order Taylor's polynomial centred at $\bar{C}^u_{SAR}(\mathbb{E}[a])$, given by

$$\bar{C}^u_{SAR} \approx K\cdot B\cdot\left(p(\mu_a)+\frac{p^{(2)}(\mu_a)\cdot\sigma^2_a}{2}\right), \tag{B.10}$$

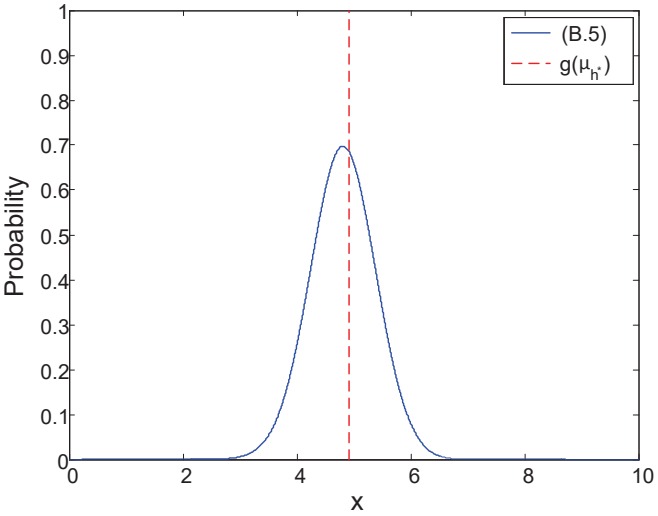

Fig. 7. Pdf of $g(|h_{k,n_k}|^2)$ versus $|h_{k,n_k}|^2$. $\frac{P_{max}}{\sigma^2}=100$ (20dB), $N=10$ and $K=10$.

$$\bar{C}_{SAR}^{u} = \frac{B(N-1)^2}{N-2} \cdot \log_2\left(1+\frac{\xi K \mathbb{H}(K)}{N-1}\right) - \frac{B\pi^2(N-1)\xi^2K^2}{12\log(2)(\xi K\mathbb{H}(K)+N-1)^2} - \frac{B(N-1)}{2\log(2)(N-2)} \cdot \frac{(c+3)d^4+2(4-c)d^3+7d^2+2d}{(d+1)^4}, \quad \text{(B.12)}$$

$$\mathbb{E}[r] = N\left[1-\frac{1}{(1-c^{-\beta})^N}\int_1^c \left(1-\frac{y^{-\beta}-\beta y^{-1}}{1-\beta}\right) d(1-y^{-\beta})^{N-1}\right] \overset{A=1-y^{-\beta}}{=} N\left[1-\frac{1}{((1-c^{-\beta})^N)(1-\beta)} \underbrace{\int_0^{1-c^{-\beta}} \left(A-\beta+\beta(1-A)^{1/\beta}\right) dA^{N-1}}_{G(A)}\right], \quad \text{(D.3)}$$

$$G(A) = (1-c^{-\beta})^{N-1}\cdot(1-c^{-\beta}-\beta+\beta c^{-1}) - \int_0^{1-c^{-\beta}} A^{N-1}dA - \beta\int_0^{1-c^{-\beta}} A^{N-1}d(1-A)^{1/\beta} = (1-c^{-\beta})^{N-1}\cdot(1-c^{-\beta}-\beta+\beta c^{-1}) - \frac{(1-c^{-\beta})^N}{N} + B_{inc}\left(1-c^{-\beta}, N, \frac{1}{\beta}\right), \quad \text{(D.4)}$$

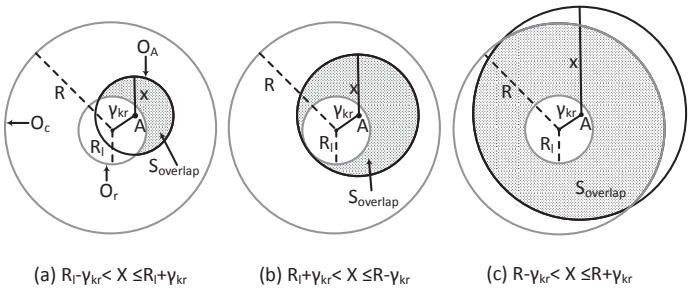

Fig. 8. Graphic illustration of $S_{overlap}$.

where

$$p(x) = \frac{1}{x}\left[\log_2(1+\xi\mu_{h^*}x) - \left(\frac{\xi^2x^2}{2(1+\xi\mu_{h^*}x)^2\log(2)}\right)\sigma_{h^*}^2\right]. \quad \text{(B.11)}$$

After some manipulation, the closed form of $\bar{C}_{SAR}^{u}$ can then be derived as (B.12), where $d = \frac{\xi\cdot K\cdot\mathbb{H}(K)}{N-1}$. For the sake of simplicity, the last term of (B.12) can be neglected since it is much smaller than the first and second terms. Thus, (22) is obtained.

Appendix C
Derivation of (34) and (35)

It is assumed that D2D pairs are distributed over a circular cell with radius R according to a homogeneous PPP Φ_A. Conditioned on the number of D2D pairs within each sub-cell, the D2D pairs are independently and uniformly distributed within each sub-cell. For $D2D_{k_r}$ within reference sub-cell l_r, the intra-cell interference is from the area between the boundary of central sub-cell circle O_r and the cell O_c. Therefore, the distance of interference link $d_{k_r,k_{l'}}$ has the following conditional cdf

$$F_{d_{k_r,k_{l'}}|\gamma_{k_r}}(x|y) = \frac{S_{overlap}}{\pi R^2 - \pi {R_l}^2}, \quad \text{(C.1)}$$

where $S_{overlap}$ is shown in Fig. 8, which is the shaded intersection area of the circle O_A with center A, radius x and the annulus interference area.

As shown in the figure, $S_{overlap}$ is a discontinuous function regarding the location of $D2D_{k_r}$, $A_{k_r}(\gamma_{k_r},\phi_{k_r})$. It can be easily observed that

$$S_{overlap} = \begin{cases} \pi x^2 - S_l, & R_l-\gamma_{k_r} < x \le R_l+\gamma_{k_r}, \\ \pi x^2 - \pi R_l^2, & R_l+\gamma_{k_r} < x \le R-\gamma_{k_r}, \\ S_c - \pi R_l^2, & R-\gamma_{k_r} < x \le R+\gamma_{k_r}, \end{cases} \quad \text{(C.2)}$$

where S_l and S_c are the intersection area of circle O_A and circle O_r and the intersection area of circle O_A and circle O_c, respectively. According to [31], the intersection area of two circles, S_{inter} is given by

$$S_{inter}(r) = \pi x^2\left(1-\tfrac{1}{\pi}\arccos\tfrac{r^2-x^2-y^2}{2xy}\right) + \arccos\tfrac{r^2+y^2-x^2}{2ry} \cdot r^2 - 2\sqrt{\tfrac{r+x+y}{2}\left(\tfrac{r+x+y}{2}-r\right)\left(\tfrac{r+x+y}{2}-x\right)\left(\tfrac{r+x+y}{2}-y\right)}. \quad \text{(C.3)}$$

Therefore, we have $S_l = S_{inter}(R_l)$ and $S_c = S_{inter}(R)$. (34) can be then obtained by combining (C.1)-(C.3).

Appendix D
Proof of Theorem 2

As $X_1,\cdots,X_N$ are i.i.d., the expectation of r was derived in Appendix B of [32] as

$$\mathbb{E}[r] = N\left(1-\int_1^c T(y)dF^{N-1}(y)\right), \quad \text{(D.1)}$$

where

$$T(y) = \frac{1}{y}\int_1^y \frac{1-x^{-\beta}}{1-c^{-\beta}}\,dx = \frac{1}{1-c^{-\beta}}\left(1 - \frac{y^{-\beta}-\beta y^{-1}}{1-\beta}\right). \tag{D.2}$$

By substituting (D.2), (42) into (D.1) and after some manipulation, we have (D.3), where $G(A)$ can be further simplified by applying integration by parts as (D.4), where $B_{inc}(x,a,b) = \int_0^x t^{a-1}(1-t)^{b-1}dt$ is the incomplete Beta function. Finally, (43) can be obtained by combining (D.3) and (D.4).

REFERENCES

[1] L. Lei, Z. Zhong, C. Lin, and X. Shen, "Operator controlled Device-to-Device communications in LTE-advanced networks," *IEEE Wireless Communications*, vol. 19, no. 3, pp. 96–104, 2012.

[2] L. Wei, R. Q. Hu, Y. Qian, and G. Wu, "Enable device-to-device communications underlaying cellular networks: challenges and research aspects," *IEEE Communications Magazine*, vol. 52, pp. 90–96, June 2014.

[3] S. Xu, K. S. Kwak, and R. Rao, "Interference-aware resource sharing in D2D underlaying LTE-A networks," *Transactions on Emerging Telecommunications Technologies*, vol. 26, no. 12, pp. 1306–1322, 2015. ett.2964.

[4] G. Fodor, E. Dahlman, G. Mildh, S. Parkvall, N. Reider, G. Miklos, and Z. Turanyi, "Design aspects of network assisted device-to-device communications," *IEEE Communications Magazine*, vol. 50, no. 3, pp. 170–177, 2012.

[5] C. Y. Wong, R. Cheng, K. Lataief, and R. Murch, "Multiuser OFDM with adaptive subcarrier, bit, and power allocation," *IEEE Journal on Selected Areas in Communications*, vol. 17, pp. 1747–1758, Oct 1999.

[6] H. Zhu and J. Wang, "Chunk-based resource allocation in OFDMA systems - part I: chunk allocation," *IEEE Transactions on Communications*, vol. 57, pp. 2734–2744, Sept 2009.

[7] Y. Li, T. Jiang, M. Sheng, and Y. Zhu, "Qos-aware admission control and resource allocation in underlay device-to-device spectrum-sharing networks," *IEEE Journal on Selected Areas in Communications*, vol. 34, pp. 2874–2886, Nov 2016.

[8] M. Sheng, Y. Li, X. Wang, J. Li, and Y. Shi, "Energy efficiency and delay tradeoff in device-to-device communications underlaying cellular networks," *IEEE Journal on Selected Areas in Communications*, vol. 34, pp. 92–106, Jan 2016.

[9] R. Zhang, X. Cheng, L. Yang, and B. Jiao, "Interference graph-based resource allocation (ingra) for D2D communications underlaying cellular networks," *IEEE Transactions on Vehicular Technology*, vol. 64, pp. 3844–3850, Aug 2015.

[10] H. Zhang, L. Song, and Z. Han, "Radio resource allocation for device-to-device underlay communication using hypergraph theory," *IEEE Transactions on Wireless Communications*, vol. 15, pp. 4852–4861, July 2016.

[11] Q. Ye, M. Al-Shalash, C. Caramanis, and J. G. Andrews, "Distributed resource allocation in device-to-device enhanced cellular networks," *IEEE Transactions on Communications*, vol. 63, pp. 441–454, Feb 2015.

[12] R. Yin, G. Yu, H. Zhang, Z. Zhang, and G. Y. Li, "Pricing-based interference coordination for D2D communications in cellular networks," *IEEE Transactions on Wireless Communications*, vol. 14, pp. 1519–1532, March 2015.

[13] N. Lee, X. Lin, J. G. Andrews, and R. W. Heath, "Power control for D2D underlaid cellular networks: Modeling, algorithms, and analysis," *IEEE Journal on Selected Areas in Communications*, vol. 33, pp. 1–13, Jan 2015.

[14] C.-H. Yu, K. Doppler, C. Ribeiro, and O. Tirkkonen, "Resource sharing optimization for device-to-device communication underlaying cellular networks," *IEEE Transactions on Wireless Communications*, vol. 10, pp. 2752–2763, Aug 2011.

[15] Z. Q. Luo and S. Zhang, "Dynamic spectrum management: Complexity and duality," *IEEE Journal of Selected Topics in Signal Processing*, vol. 2, pp. 57–73, Feb 2008.

[16] W. Yu and R. Lui, "Dual methods for nonconvex spectrum optimization of multicarrier systems," *IEEE Transactions on Communications*, vol. 54, pp. 1310–1322, July 2006.

[17] Y. Li, M. Sheng, C. W. Tan, Y. Zhang, Y. Sun, X. Wang, Y. Shi, and J. Li, "Energy-efficient subcarrier assignment and power allocation in ofdma systems with max-min fairness guarantees," *IEEE Transactions on Communications*, vol. 63, pp. 3183–3195, Sept 2015.

[18] R. Tang, J. Zhao, H. Qu, and Z. Zhang, "User-centric joint admission control and resource allocation for 5G D2D extreme mobile broadband: A sequential convex programming approach," *IEEE Communications Letters*, vol. 21, pp. 1641–1644, July 2017.

[19] H. Tang and Z. Ding, "Mixed mode transmission and resource allocation for D2D communication," *IEEE Transactions on Wireless Communications*, vol. 15, pp. 162–175, Jan 2016.

[20] D. T. Ngo, S. Khakurel, and T. Le-Ngoc, "Joint subchannel assignment and power allocation for ofdma femtocell networks," *IEEE Transactions on Wireless Communications*, vol. 13, pp. 342–355, January 2014.

[21] D. Burghal and A. F. Molisch, "Efficient channel state information acquisition for device-to-device networks," *IEEE Transactions on Wireless Communications*, vol. 15, pp. 965–979, Feb 2016.

[22] H. Min, J. Lee, S. Park, and D. Hong, "Capacity enhancement using an interference limited area for device-to-device uplink underlaying cellular networks," *IEEE Transactions on Wireless Communications*, vol. 10, pp. 3995–4000, Dec 2011.

[23] A. Prasad, A. Kunz, G. Velev, K. Samdanis, and J. Song, "Energy-efficient d2d discovery for proximity services in 3gpp lte-advanced networks: Prose discovery mechanisms," *IEEE Vehicular Technology Magazine*, vol. 9, pp. 40–50, Dec 2014.

[24] J. Wang and L. Milstein, "CDMA overlay situations for microcellular mobile communications," *IEEE Transactions on Communications*, vol. 43, pp. 603–614, Feb 1995.

[25] J. Jang and K. B. Lee, "Transmit power adaptation for multiuser OFDM systems," *IEEE Journal on Selected Areas in Communications*, vol. 21, pp. 171–178, Feb 2003.

[26] Y. Kai and H. Zhu, "Resource allocation for multiple-pair D2D communications in cellular networks," in *2015 IEEE International Conference on Communications (ICC)*, pp. 2955–2960, June 2015.

[27] E. Biglieri, J. Proakis, and S. Shamai, "Fading channels: information-theoretic and communications aspects," *IEEE Transactions on Information Theory*, vol. 44, pp. 2619–2692, Oct 1998.

[28] W. Yu and J. M. Cioffi, "Constant-power waterfilling: performance bound and low-complexity implementation," *IEEE Transactions on Communications*, vol. 54, pp. 23–28, Jan 2006.

[29] A. Papoulis, *Probability, Random Variables, and Stochastic Processes*. Communications and signal processing, McGraw-Hill, 1991.

[30] G. George, R. K. Mungara, A. Lozano, and M. Haenggi, "Ergodic spectral efficiency in MIMO cellular networks," *IEEE Transactions on Wireless Communications*, vol. 16, pp. 2835–2849, May 2017.

[31] L. Dai, "A comparative study on uplink sum capacity with co-located and distributed antennas," *IEEE Journal on Selected Areas in Communications*, vol. 29, pp. 1200–1213, June 2011.

[32] Y. Y. Zaliapin, I. V.and Kagan and F. P. Schoenberg, "Approximating the distribution of pareto sums," *pure and applied geophysics*, vol. 162, no. 6, pp. 1187–1228, 2005.

Yuan Kai (S'15-M'18) received the B.Eng. degree in Electronic and Communications Engineering from the University of Bristol, Bristol, U.K., in 2011, and the M.Sc degree and Ph.D. degree in Electronic Engineering from the School of Engineering and Digital Arts, University of Kent, Canterbury, in 2012 and 2018, respectively.

His research focuses on performance analysis and algorithm design for wireless communication systems, with special interests in vehicle-to-x communications, device-to-device communications, internet of things and mobile edge computing.

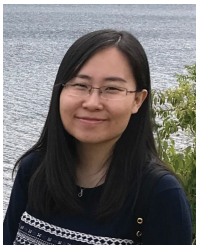

Junyuan Wang (S'13-M'15) received the B.S. degree in Communications Engineering from Xidian University, Xi'an, China, in 2010, and Ph.D. degree in Electronic Engineering from City University of Hong Kong, Hong Kong, China, in 2015. She was a Research Associate at the University of Kent from 2015 to 2017.

She is currently a Lecturer (Assistant Professor) at the Department of Computer Science, Edge Hill University, Ormskirk, U.K. Her research focuses on performance analysis and algorithm design for wireless communication systems with special interests in massive MIMO, distributed antenna systems/C-RAN and device-to-device communications. She was a co-recipient of the Best Student Paper Award at the IEEE 85th Vehicular Technology Conference (VTC) - Spring 2017.

Huiling Zhu (SM17) received the B.S degree from Xidian Univeristy, Xian, China, and the Ph.D. degree from Tsinghua University, Beijing, China. She is currently a Reader (Associate Professor) in the School of Engineering and Digital Arts, University of Kent, Canterbury, United Kingdom. Her research interests are in the area of wireless communications, covering topics such as radio resource management, MIMO, cooperative communications, device-to-device communications, Cloud RAN, and small cells and heterogeneous networks. She received the best paper award from IEEE Globecom2011. She has participated in a number of European and industrial projects in these topics and was holding European Commission Marie Curie Fellowship from 2014 to 2016. She has served as the Publication Chair for IEEE WCNC 2013, Operation Chair for IEEE ICC 2015, Symposium Co-Chair for IEEE Globecom 2015 and IEEE ICC 2018, and Track Co-Chair of IEEE VTC2016-Spring and VTC2018-Spring. Currently, she serves as an Editor for IEEE Transactions on Vehicular Technology.

Jiangzhou Wang (F17) is currently a professor and the former Head of the School of Engineering and Digital Arts, University of Kent, United Kingdom. He has authored over 300 papers in international journals and conferences in the areas of wireless mobile communications and three books.

He is a Fellow of Royal Academy of Engineering (UK), an IEEE Fellow and IET Fellow. He received the Best Paper Award from the 2012 IEEE GLOBECOM and was an IEEE Distinguished Lecturer from 2013 to 2014. He is the TPC Chair of IEEE ICC2019, Shanghai. He was the Executive Chair of the ICC2015 in London and the TPC Chair of the 2013 IEEE WCNC (WCNC2013). He was an Editor for IEEE Transactions on Communications from 1998 to 2013 and was a Guest Editor for IEEE Journal on Selected Areas in Communications, IEEE Communications Magazine, and IEEE Wireless Communications. His research interests include massive MIMO, C-RAN, NOMA, and D2D communications.